Western diet-induced increase in colonic bile acids compromises epithelial barrier in nonalcoholic steatohepatitis

Biki Gupta[1], Yunshan Liu[2], Daniel M. Chopyk[2], Ravi P. Rai[1], Chirayu Desai[4], Pradeep Kumar[1], Alton B. Farris[3], Asma Nusrat[5], Charles A. Parkos[5], Frank A. Anania[6], Reben Raeman[1,7]*

Division of Experimental Pathology[1], Department of Pathology, University of Pittsburgh, Pittsburgh, PA; Division of Digestive Diseases[2]; Department of Pathology and Laboratory Medicine[3], Department of Medicine, Emory University, Atlanta, GA; Microbiology and Immunology[4], P. D. Patel Institute of Applied Sciences, Charotar University of Science and Technology, Gujarat, India; Department of Pathology[5], University of Michigan, Ann Arbor, MI; Division of Gastroenterology and Inborn Error Products[6], Food and Drug Administration, Silver Spring, MD; Pittsburgh Liver Research Center[7], University of Pittsburgh Medical Center and University of Pittsburgh School of Medicine, Pittsburgh, PA USA.

***Corresponding Author:**
Reben Raeman, M.S., Ph.D.
Assistant Professor
200 Lothrop Street, S408 BST,
Pittsburgh, PA 15261
Phone: 412-648-2021
Email: reben.raeman@pitt.edu

Running title: *Bile acids compromise intestinal epithelial barrier in NASH*

Keywords*:* Bile acids, tight junction, intestinal permeability, microbiome, NAFLD, NASH

Abbreviations*:* Metabolic Syndrome, MetS; non-alcoholic fatty liver disease, NAFLD; non-alcoholic steatohepatitis, NASH

Conflict of interest: All authors declare no conflicting interests.

Funding: Research reported in this publication was supported by the National Institute of Diabetes and Digestive and Kidney Diseases of the National Institutes of Health under award number K01DK110264 to RR, and DK072564 and DK061379 to CP, and by the National Institute on Alcohol Abuse and Alcoholism award number F31AA024960 to DMC. The content is solely the responsibility of the authors and does not necessarily represent the official views of the National Institutes of Health, the US Food and Drug Administration, the US Department of Health and Human Services, or the US Government.

Author Contributions.

R.R. conceived the project, designed and performed experiments, analyzed data, wrote the manuscript

F.A.A. provided valuable suggestions and scientific editing

B.K. maintained mouse colonies, performed experiments

Y.L. maintained mouse colonies, collected metabolic data, performed experiments

D.C. provided assistance with the *in vitro* permeability studies

R.P.R. maintained mouse colonies, performed experiments

C.D. analyzed microbiota data

P.K. provided valuable suggestions

A.B.F NASH-CRN scoring

C.A.P. provided valuable suggestions, provided knockout mice.

A.S.N. provided valuable suggestions.

ABSTRACT

There is compelling evidence implicating intestinal permeability in the pathogenesis of nonalcoholic steatohepatitis (NASH), but the underlying mechanisms remain poorly understood. Here we examined the role of bile acids (BA) in western diet (WD)-induced loss of colonic epithelial barrier (CEB) function in mice with a genetic impairment in intestinal epithelial barrier function, junctional adhesion molecule A knockout mice, *F11r*$^{-/-}$. WD-fed knockout mice developed severe NASH, which was associated with increased BA concentration in the cecum and loss of CEB function. Analysis of cecal BA composition revealed selective increases in primary unconjugated BAs in the WD-fed mice, which correlated with increased abundance of microbial taxa linked to BA metabolism. *In vitro* permeability assays revealed that chenodeoxycholic acid (CDCA), which was elevated in the cecum of WD-fed mice, increased paracellular permeability while the BA-binding resin sevelamer hydrochloride protected against CDCA-induced loss of barrier function. Sequestration of intestinal BAs by *in vivo* delivery of sevelamer to WD-fed knockout mice attenuated colonic mucosal inflammation and improved CEB. Sevelamer also reduced hepatic inflammation and fibrosis, and improved metabolic derangements associated with NASH. Collectively, these findings highlight a hitherto unappreciated role for BAs in WD-induced impairment of the intestinal epithelial barrier in NASH.

INTRODUCTION

Nonalcoholic fatty liver disease (NAFLD) can be considered the hepatic manifestation of the metabolic syndrome (MetS), which is associated with chronic diseases including type 2 diabetes mellitus (DM), essential hypertension, dyslipidemia, obesity, and hypothyroidism (1-3). An estimated 30-40% of Americans have increased nonalcohol-related free fatty acid (FFA) and triglyceride (TGs) deposition in the hepatocytes, termed bland steatosis, or nonalcoholic fatty liver (NAFL) (4, 5). In approximately one-fifth of NAFL patients, disease progression can result in nonalcoholic steatohepatitis (NASH), which is characterized by increased inflammation and mild to moderate fibrosis. A subset of NASH patients is at significantly higher risk of developing cirrhosis, and ultimately hepatocellular carcinoma (HCC) (1, 2). Despite ongoing research, mechanisms leading to NAFLD progression remain poorly understood, and no effective treatment for NASH exists, nor do we have a therapy to prevent disease progression.

Recent advances in our understanding of NASH pathogenesis underscore the contribution of the gut-liver axis in NAFLD progression. The concept of gut-liver-axis in NAFLD progression emerged from human and animal studies demonstrating an association between increased intestinal epithelial permeability and serum endotoxin level, a potent driver of hepatic inflammation (6-8). We have recently demonstrated that western diet (WD) feeding of mice with a compromised intestinal epithelial barrier (junctional adhesion molecule A knockout mice, *F11r*$^{-/-}$), results in the rapid development of steatohepatitis with significant fibrosis (9). NAFLD progression in this model of compromised intestinal epithelial barrier correlated with further increase in intestinal epithelial permeability to gut bacterial products as well as perturbations in gut microbial composition (9). While this study confirmed the role of intestinal epithelial permeability and associated microbial dysbiosis in NAFLD progression, the mechanisms by which WD compromises intestinal epithelial barrier remain unclear.

Bile acids (BA) are amphipathic sterols synthesized in the liver from cholesterol, stored in the gall bladder, and released in the small intestine postprandially to facilitate the

absorption of dietary fat, cholesterol and fat-soluble vitamins (10, 11). BAs secreted into the intestine are reabsorbed (~90 - 95%), and recirculated to the liver via the entero-hepatic circulation. While the majority of BA reuptake occurs in the ileum, a small percentage of BAs are also reabsorbed in the colon. Colonic absorption of BAs is facilitated by gut microbiota, which convert the conjugated BAs into more hydrophobic molecules to enable their reabsorption by passive diffusion across cell membrane (12-14). The entero-hepatic cycling of BAs is a highly efficient and tightly orchestrated process that not only provides an effective recycling mechanism to conserve and maintain a constant BA pool, but also serves as a mechanism to restrict BAs to the intestinal and hepatobiliary compartments (15). Disruption of this process, primarily due to BA malabsorption or excessive biotransformation by gut microbiota, can increase the passage of BAs to the colon (12, 16-18). Colonic epithelial cells are susceptible to BA induced cytotoxicity, and both *in vitro* and *in vivo* studies demonstrate that micromolar concentrations of BA can potentially compromise the integrity of the intestinal epithelial barrier (19-25). The role of BAs in WD-induced loss of intestinal epithelial barrier function in NASH is poorly defined, but a recent study reporting increased fecal BA concentrations in NASH patients (26), suggests a role for BAs in promoting colonic epithelial permeability in NASH.

The present study was designed to examine the role of BA in WD-induced impairment of intestinal epithelial barrier function in WD-fed *F11r*$^{-/-}$ mice, which develop severe steatohepatitis within 8 weeks of feeding a WD (9). Our results provide compelling evidence for a novel mechanism whereby WD-induced increases in the passage of primary, hydrophobic BA, CDCA to the colon compromises colonic epithelial barrier. We demonstrate that the BA-binding resin sevelamer hydrochloride attenuates NAFLD progression by protecting mice from BA-induced loss of colonic epithelial barrier function. In the light of recent reports implicating gut-derived antigens in promoting progression of NAFL to NASH, our findings have important clinical implications for the treatment of NASH.

MATERIALS AND METHODS

Mice. Junctional adhesion molecule A (JAM-A) knock out mice (*F11r*$^{-/-}$) were generated as previously described (9). Mice were bred and maintained at Emory University and the University of Pittsburgh Divisions of Animal Resources. All animal studies were approved by Institutional Animal Care and Use Committees.

BA feeding experiment: C57BL/6 mice were fed CDCA (3mg/gm body weight, Millipore Sigma, St. Louis, MO) mixed with FITC conjugated dextran (4 kDa) (0.6 mg/gm body weight, Millipore Sigma, St. Louis, MO) solution by oral gavage following a 6 hr fast. After 3 h, blood was collected and fluorescence intensity was measured using Fluorescence Spectrophotometer (Synergy 2, Biotek, Winooski, VT) as described previously (9).

Diet and feeding studies: Five to six-week-old male *F11r*$^{-/-}$ mice were fed a ND or WD *ad libitum* for twelve-weeks as described previously(9). After 12 weeks of feeding, mice were fed either ND or WD alone (control) or ND or WD mixed with sevelamer hydrochloride for four-weeks. The western diet (WD) consisted of 0.2% cholesterol, 20% protein, 43% CHO, 23% fat (6.6% trans-fat), and 2.31% fructose (TD.130885; Harlan Laboratories)(9). The normal diet (ND) is the standard mouse chow that contains 16% protein, 61% carbohydrate, and 7.2% fat.

Histopathology. Hematoxylin and eosin (H&E) and Sirius Red staining were performed on formalin-fixed liver and colon tissue sections, as previously reported [4]. A Zeiss Light Microscope (Zeiss, Jena, Germany) was employed to obtain photomicrographs of the histologic sections.

Bile acid analysis. Bile acids extracted from liver and cecal content were quantified using liquid chromatography-mass spectrometry (LC-MS) analysis. Briefly, the liver samples were homogenized in PBS, and cecal samples were sonicated in PBS. Samples were deproteinized with acetonitrile, and centrifuged; subsequently, the supernatants were lyophilized under nitrogen, and solvated in a 1:1 (v/v) mixture of methanol and water. LC-MS analysis was carried out on the SCIEX 5500 QTRAP LC-MS system

(SCIX, Framingham, MA). Analyses of all samples were performed using a C18 reverse phase HPLC column (Thermo Fisher Scientific). Multiquant 3.0.2 software was used for data processing and quantification.

Cell culture and *in vitro* permeability assay. Caco2 cells were purchased from American Type Culture Collection (ATCC, Manassas, VA). Cells were maintained in DMEM supplemented with 10% FBS, 1% penicillin-streptomycin and 1 mmol/L sodium pyruvate as described previously (27).

For the *in vitro* permeability assay, Caco2 cells (passage number 23–35) were cultured in 6- or 12-well trans-well chambers (Corning, NY, USA) at a density of 4 x 10^4 cells/cm^2 for 21 days as described previously (27). Fully differentiated Caco-2 cell monolayers were treated with 20 μM individual BAs or BAs premixed with 0.2 M sevelamer. FITC conjugated-dextran (4 kDa) (Millipore Sigma, St. Louis, MO) dissolved in Hanks' balanced salt solution (HBSS) was added to the apical compartment and incubated for 2 h in a tissue culture incubator. CA, CDCA, TCA and TDCA were dissolved in HBSS, while LCA was dissolved in methanol and then diluted with HBSS. At the end of the study, transepithelial electrical resistance (TEER) was measured using a Millicell-ERS volt-ohm meter (Millipore, Temecula, CA, USA). Media from the basal compartments was collected and fluorescent intensity was measured using Fluorescence Spectrophotometer (Synergy 2, Biotek, Winooski, VT). FITC-dextran concentrations were determined from a standard curve generated by serial dilutions of 4 kDa FITC-dextran.

Immunofluorescence microscopy. Liver and intestinal cryosections were stained for immunofluorescence (IF) microscopy as described previously [4]. Cryosections were visualized using an Axioskop 2 plus microscope (Zeiss, Jena, Germany). The antibodies used for IF staining were obtained from ThermoFisher Scientific (Rockford, IL).

Serological analysis. AST and ALT Activity Assay Kits (Sigma-Aldrich, St. Louis, MO) were used to estimate serum alanine aminotransferase (ALT) and aspartate aminotransferase (AST) concentrations.

Glucose tolerance test and insulin tolerance test. Glucose tolerance test (GTT) and insulin tolerance test (ITT) were conducted at 16 weeks of WD feeding, as previously reported [4]. A hand-held glucometer (Freestyle Flash, Abbott Laboratories, Abbott Park, IL) was used to determine the blood glucose concentration.

Quantitative real-time PCR. Total RNA was isolated from liver, followed by cDNA synthesis and qRT-PCR, based on previously described methods [4]. All data were normalized against 18S rRNA and were reported as fold change in gene expression as compared to those in ND-fed control mice.

Quantification of bacteria in the liver by RT-PCR

Total DNA from liver tissue was extracted using the QIAamp DNA Stool Mini kit (QIAGEN, GmbH, Germany) according to the manufacturer's instructions.

Statistical analysis. ANOVA, in conjunction with post-hoc analysis for multiple group comparisons, was used to analyze statistical differences. The data reported were from three independent experiments. A p value < 0.05 was considered statistically significant.

RESULTS

NASH development in WD-fed mice is associated with increased BAs in the cecum and alterations in the composition of the cecal BA pool. To induce NASH, *F11r*$^{-/-}$ mice were fed a WD for 16 weeks, *F11r*$^{-/-}$ mice fed a ND served as controls. WD-fed *F11r*$^{-/-}$ mice developed key histological features of NASH including hepatic steatosis with increased accumulation of triglycerides in hepatocytes, increased immune cell infiltration, and increased fibrosis in the perivascular and perisinusoidal regions (Fig 1A-B). Increased collagen deposition in the liver of WD-fed *F11r*$^{-/-}$ mice correlated with a significant increase in α smooth muscle actin (SMA) mRNA transcripts, a key hepatic stellate cell (HSC) activation marker (28), as well as mRNA transcripts for tissue inhibitors of metalloproteinase (TIMP)-1 and collagen I, [αI and αII] (Fig. 1B, C-F). Serum aspartate aminotransferase (AST) and alanine aminotransferase (ALT) levels were also

247 significantly higher in WD-fed mice compared to levels in the ND-fed mice
248 demonstrating severe hepatic injury in these mice (Fig. 1G-H).
249
250 To determine whether NASH development in WD-fed *F11r*$^{-/-}$ mice was associated with
251 increased passage of BAs to the cecum, we quantified total BAs in the cecal content. As
252 seen in Fig. 1I, the total cecal BA concentration in WD-fed mice was two-fold higher
253 relative to the ND-fed mice. Analysis of the BA composition by liquid chromatography-
254 mass spectrometry (LC-MS) revealed that WD consumption increased BAs with high
255 affinity for farnesoid X receptor (FXR): chenodeoxycholic acid (CDCA), cholic acid
256 (CA), lithocholic acid (LCA), as well as BAs, that are FXR antagonists: α and β
257 muricholic acid (MCA), and urodeoxycholic acid (UDCA) (Fig. 1J-K). Concentration of
258 conjugated BAs taurocholic acid (TCA), taurochenodesoxycholic acid (TCDCA) and
259 tauroursodeoxycholic acid (TUDCA) were also significantly higher in the WD-fed mice.
260 The colonic BAs in ND-fed mice consisted mainly of primary unconjugated BAs except
261 for the secondary BA deoxycholic acid (DCA). Together, these data demonstrate that
262 WD consumption not only increases the passage of BAs to the cecum, but also alters the
263 composition of cecal BA.
264
265 ***Sevelamer protects the epithelium from BA-induced loss of epithelial barrier.*** To
266 determine whether the BAs that were increased in the cecum of WD-fed mice promoted
267 epithelial permeability, we examined effects of BAs on permeability across monolayers
268 of Caco2 cells in vitro, a well-established model of human intestinal epithelial barrier
269 function (29). Caco2 cell monolayers grown on transwell inserts were treated with
270 specific BAs that were differentially represented in the cecal content of WD-fed *F11r*$^{-/-}$
271 mice and change in permeability was determined by paracellular flux of 4kDa FITC-
272 Dextran. As shown in Fig. 2A-B, CDCA, but not CA, TCA, TDCA or LCA, significantly
273 increased the paracellular flux of FITC-dextran. The CDCA-induced increase in
274 paracellular permeability correlated with a significant decrease in TEER, consistent with
275 CDCA induced impairment of barrier function in Caco2 cells (Fig. 2C-D). To determine
276 whether sevelamer, which binds and sequesters BAs (30), protects the epithelial barrier
277 from CDCA-induced loss of barrier function, we treated Caco2 monolayers with CDCA

premixed with sevelamer. As shown in Fig. 2A-B, CDCA premixed with sevelamer did not increase the paracellular flux of FITC-dextran across the Caco2 cell monolayers, and did not reduce TEER, suggesting that sevelamer neutralizes the effect of CDCA on Caco2 monolayers. To determine whether CDCA induced gut permeability *in vivo*, we measured intestinal permeability in CDCA-fed mice using the FITC-dextran permeability assay. As shown in Fig. 2E, oral gavage of CDCA induced a 9-fold increase in paracellular flux of 4kDa FITC-Dextran. Together, these data suggest that WD-induced increase in the passage of CDCA to the cecum of *F11r*$^{-/-}$ mice impaired colonic epithelial barrier.

Sequestration of BAs improves WD-induced disruption of colonic epithelial barrier. Next, we sought to determine whether sequestration of BAs would protect *F11r*$^{-/-}$ mice from WD-induced loss of colonic epithelial barrier. To address this question, a cohort of *F11r*$^{-/-}$ mice fed a ND or WD for 12-weeks were administered sevelamer mixed with diet for an additional four weeks (Fig. 3A). At the end of the study we analyzed the respective BA composition of the cecal contents, which revealed a significant increase in BAs in the mice fed a WD mixed with sevelamer compared to the cohort of mice fed the WD alone; however, no differences in the concentration of total BAs were observed between mice fed a ND or ND mixed with sevelamer (Fig. 3B). Analysis of the composition of the BA in the cecal content revealed a significant increase in the concentration of CDCA, CA, LCA, TCA TLCA, and TCDCA in sevelamer-treated ND and WD fed mice demonstrating that sevelamer sequestered both hydrophobic and hydrophilic BAs (Fig. 3C).

To determine whether sequestration of intestinal BAs improves colonic epithelial barrier, we examined colonic expression and distribution of the tight junction (TJ) proteins, occludin and zonula occludens (ZO)-1 using confocal laser scanning microscopy. As evident in the photomicrograph (Fig. 3D-G and Supp. Fig. 1A-B), compared with ND fed mice, occludin and ZO-1 expression were markedly reduced in the colonic mucosa of WD-fed mice. Sevelamer treatment restored WD-induced reduction and redistribution of occludin and ZO-1 in the colonic mucosa of mice fed a WD. No significant differences in

occludin and ZO-1 expression were observed between mice fed a ND or ND mixed with sevelamer (Supp. Fig. 1A-B). Together, these data suggest that sequestration of BAs improves WD-induced loss of colonic epithelial barrier by restoring structural integrity of epithelial TJs.

Bile acid sequestration attenuates WD-induced mucosal inflammation. As seen in Fig. 4A and Supp. Fig. 2A, WD consumption resulted in severe colonic mucosal inflammation indicated by increased infiltration of immune cells in the mucosa. Further analysis revealed marked increase in the infiltration of Ly6G+ neutrophils and monocytes as well as myeloperoxidase (MPO) expressing cells in the colonic mucosa of WD-fed *F11r*$^{-/-}$ mice relative to ND-fed mice (Fig. 4B-C and Supp. Fig. 2B-C). The transcript levels of proinflammatory cytokines, TNFα and IL1β were significantly higher in the colonic mucosa of WD-fed mice relative to the ND-fed mice demonstrating that WD-consumption resulted in severe mucosal inflammation in these mice (Fig. 4D-E). The transcript levels of monocyte chemoattractant protein (MCP)-1, C-C chemokine receptor (CCR)-2 and F4/80 remained unchanged (Supp. Fig. 2D-F). Sevelamer administration attenuated WD-induced mucosal inflammation as evident by a marked reduction in immune cell infiltration in the colonic mucosa, and a significant decrease in transcript levels of TNFα (Fig. 4A-D). Levels of IL1β, however, remained unchanged (Fig. 4E).

Sequestration of excreted BAs attenuates hepatic inflammation and fibrosis in WD-fed mice. To determine whether administration of sevelamer improved NASH we examined histological and biochemical features of NASH in sevelamer treated WD-fed *F11r*$^{-/-}$ mice. In agreement with a recent study (31), sevelamer markedly reduced hepatic steatosis, inflammation, and fibrosis in the WD-fed mice (Fig. 5A-P and Supp. Fig. 3A-C). Improvement in hepatic inflammation in sevelamer treated WD-fed mice was confirmed by a significant reduction in serum AST and ALT levels (Fig. 5B-C), and reduction in hepatic TNFα, IL1β, and IL6 levels (Fig. 5D-F). Administration of sevelamer significantly decreased mRNA transcripts of αSMA, TIMP-1, and collagen I [αI and αII] (Fig. 5H-K) demonstrating a significant reduction in HSC activation and collagen deposition in WD-fed mice. Sevelamer treatment also reduced hepatic

macrophage infiltration (Fig. 5L and Supp. Fig. 3C), which correlated with a significant decrease in F4/80, MCP-1, CD68, and CCR2 transcripts. Together, these data demonstrate that administration of sevelamer not only attenuated hepatic steatosis and inflammation, but also ameliorated hepatic fibrosis in WD-fed mice.

Sequestration of excreted BAs improves metabolic parameters in WD-fed mice. Examination of metabolic parameters in sevelamer treated mice revealed a significant reduction in body weight in WD-fed *F11r*$^{-/-}$ mice, but not in ND-fed mice (Fig. 6A). Reduction in body weight was most significant in the first two weeks of treatment, after which body weight of sevelamer treated WD-fed mice remained stable (Fig. 6A). Sevelamer treatment significantly decreased liver weight/body weight and visceral fat weight/body weight ratios respectively (Fig. 6B-C). While sevelamer treatment reduced the liver weights of WD-fed mice compared to the ND-fed mice, visceral fat weight remained higher (Fig. 6B-C) in the former. Even after four-weeks of sevelamer treatment, visceral fat weight of WD-fed mice remained two-fold higher than the ND-fed mice (Fig. 6C). We observed improved metabolic parameters in sevelamer treated WD-fed mice including improved glycemic control and insulin sensitivity (Fig. 6A-E). We observed no significant differences in metabolic parameters between mice fed a ND or ND and sevelamer (Fig. 6A-E). Sevelamer treatment significantly reduced serum cholesterol levels to levels comparable to those recorded in the ND-fed mouse cohort (Fig. 6F) suggesting that sequestration of intestinal BA improves whole body cholesterol metabolism in WD-fed mice. Sevelamer treatment also reduced hepatic fat deposition in the WD-fed mice (Fig. 6G). No differences in average calorie intake was observed between control and sevelamer treated WD-fed mice (Fig. 6H).

Intestinal BA sequestration reverses WD-induced alteration in hepatic BA composition and increases hepatic BA synthesis. To understand the mechanism of sevelamer-mediated improvement in metabolic parameters, we examined hepatic BA composition in sevelamer treated WD-fed *F11r*$^{-/-}$ mice. As shown in Fig. 7A-B, WD consumption did not increase total BA concentrations in the liver; rather, it altered hepatic BA composition. WD consumption significantly increased TCDCA, but decreased TDCA in

the liver (Fig. 7B). Sevelamer treatment did not change total BA concentration in the liver, but decreased βMCA concentration and restored TCDCA concentrations to that seen in the livers of ND-fed mice (Fig. 7A-B). To understand the effect of sevelamer on hepatic BA synthesis, we analyzed key enzymes that regulate BA biosynthesis in the liver. As shown in Fig. 7C-E, sevelamer treatment significantly increased the expression of key enzymes involved in the classical and alternative BA synthesis pathways, cholesterol 7α-hydroxylase (*CYP7A1*), sterol 27-hydroxylase (*CYP27A1*) and oxysterol 7α-hydroxylase (*CYP7B1*) transcripts. Together, these data suggest that sequestration of BAs activates both classic and alternative BA synthesis pathways in the liver without altering hepatic BA pool size.

WD increases the abundance of microbial taxa associated with BA metabolism. Since microbiota play a significant role in metabolism, and the absorption and excretion of BAs (32), we analyzed cecal mucosa-associated microbiota by 16S rRNA sequencing followed by phylogenetic analyses and a comparison of the microbial community structure using the unweighted UniFrac algorithm as described previously (9). As seen in Fig. 8A-B, WD consumption decreased diversity and altered composition of colonic mucosa-associated microbial composition. At the order level, WD consumption resulted in the expansion of *Bacteroidales* and *Clostridiales*, major gut microbial taxa with bile salt hydrolase activity (33, 34); as well as *Desulfovibrionales*, a bacterial taxa associated with colitis (35); and *Deferribacterales* (Fig. 8C). At the family level, WD increased the abundance of *Bacteroidaceae, Odoribacteraceae* and *Desulfovibrionaceae*, but decreased S24-7 (Fig. 8D). Sevelamer treatment did not significantly alter the microbial composition in the ND or WD fed mice, except for a significant reduction in the abundance of *Deferribacteraceae* in the WD-fed mice. Together, these data suggest a link between increased BA metabolizing bacterial taxa in the cecum and increased unconjugated BAs in the cecal content of WD-fed mice.

DISCUSSION

In the present study, we provide a potential mechanistic explanation underpinning the loss of intestinal epithelial barrier function in NASH by demonstrating that WD-induced

increase in the primary BA, CDCA in the cecum disrupts the colonic epithelial barrier in mice that ultimately develop severe NASH. We show that the effect of CDCA on colonic mucosa was attenuated by oral administration of the BA binding resin sevelamer, secondary to a marked decrease in hepatic inflammation and fibrosis. Collectively our data implicate CDCA as a contributing factor in WD-induced loss of colonic epithelial barrier in NASH, and provide evidence that BA binding resins may represent a promising treatment for NASH. Furthermore, hepatic injury in *F11r*$^{-/-}$ mice following 16 weeks of WD consumption recapitulates key physiological, metabolic, and histological features of human NASH with fibrosis, demonstrating the utility of this accelerated rodent model of progressive NASH for preclinical studies.

Under normal physiological conditions, only a small amount of BA reaches the colon, where it is metabolized by resident microbiota to facilitate reabsorption and excretion in the stool. Higher concentrations of BAs in the colon, however disrupt colonic epithelial barrier integrity ultimately resulting in loss of barrier function (19-22). The extent of BA-induced cytotoxicity and subsequent tissue injury depends on the conjugation status, concentration, and the duration of exposure (36). At abnormally high concentrations, BAs disrupt cell membranes, cause oxidative/nitrosative stress, and apoptosis (23, 36, 37). By contrast, prolonged exposure to high concentrations of BAs results in genomic instability and apoptosis resistance, which can lead to the development of cancer (38, 39). Our results demonstrate an association between elevated cecal BA levels, including the highly cytotoxic primary BA, CDCA, and colonic epithelial injury in WD-fed mice. As demonstrated by other investigators, CDCA is a potent inducer of epithelial permeability (21, 24, 25). This together with our data from *in vitro* permeability assay and *in vivo* BA-feeding study implicate CDCA as a major player in driving intestinal epithelial permeability, and ultimately NAFLD progression. While CA did not induce epithelial permeability in our *in vitro* permeability assay, CA is well known to be highly cytotoxic to intestinal epithelial cells (23), and conceivably chronic exposure to high concentration of CA may contribute to colonic tissue injury. Suggesting that similar mechanisms may be at play in human NASH, a recent study reported increased fecal BA concentrations in NASH patients, and interestingly NASH patients also present with significantly higher

levels of CA and CDCA in the stool (26). Collectively, these results suggest that diet-induced changes in the composition of the cecal BA pool could contribute to increased intestinal epithelial permeability that would promote NAFLD progression to NASH with fibrosis (9).

Sevelamer hydrochloride has profound BA-binding abilities due to its unique cooperative binding property that enables it to bind more hydrophobic BAs, thereby acting as a sink for more BA binding, ultimately leading to net excretion of BAs in the stool (30). A significant 7-fold increase in CDCA and 3-fold increase in CA in the cecum content of sevelamer treated WD-fed mice is a testament to the effectiveness of sevelamer in sequestering these two cytotoxic BAs from the colon. This correlated with a marked reduction in colonic mucosal inflammation and restoration of colonic epithelial barrier in sevelamer treated WD-fed mice suggesting that the ability of sevelamer to bind and neutralize excess BAs in the colon played a central role in protecting the colonic mucosa from the harmful effect of cytotoxic BAs. Collectively these data further establish the role of BAs in diet-induced impairment of colonic epithelial barrier in NASH.

Microbial metabolism of BAs not only increases the diversity and hydrophobicity of the BA pool, but also facilitates passive absorption and excretion of BAs (12). Most gut microbial taxa including *Lactobacilli*, *Bifidobacteria, Clostridium,* and *Bacteroides* have bile salt hydrolase activity and can deconjugate BAs (33, 40, 41). BA deconjugation, however prevents active reuptake of BAs via the ASBT transporter responsible for the majority of BA reuptake in the terminal ileum resulting in increased passage of BAs to the colon (15). Accordingly, in the absence of bacteria in the germ-free or antibiotic-treated mice, BA pool consists of primary conjugated BAs, and fecal excretion of BAs is decreased in germ-free mice (32, 40). In agreement with these findings, increase in unconjugated BAs in the colon of WD-fed mice was associated with increased abundance of *Clostridium* and *Bacteroides* implicating their potential role in increasing unconjugated BAs in the colon of WD-fed mice. Likewise, increase in cecal LCA also correlated with higher abundance of *Clostridium*, which are among a small number of intestinal anaerobes with 7- dehydratase activity, the enzyme required for the production

of DCA and LCA (12, 33, 42). Despite marked improvement in colonic mucosal injury in sevelamer treated mice, sevelamer treatment did not significantly alter the abundance of taxa belonging to either *Clostridium* or *Bacteroides*. Increase in unconjugated BAs in the cecum of sevelamer treated WD-fed mice suggest that the ability of sevelamer to sequester and neutralize the cytotoxic effect of BAs protected mucosa from BA-induced injury.

Improvement in metabolic derangements associated with NAFLD and NASH in the sevelamer treated WD-fed mice may be explained in part by increased hepatic BA biosynthesis, which is the major pathway for catabolizing dietary cholesterol and maintaining whole body-cholesterol homeostasis (10, 11). Increased BA biosynthesis in transgenic mice overexpressing *CYP7A1*, the rate-limiting enzyme in hepatic BA biosynthesis, improves metabolic homeostasis, high-fat diet-induced obesity, and insulin resistance (43, 44). In agreement with these reports, our data demonstrate a significant increase in hepatic *CYP7A1* expression, which was also associated with a significant decrease in serum cholesterol in sevelamer-treated WD-fed mice. Sevelamer treatment also increased hepatic *CYP27A1* expression in the WD-fed mice suggesting that intestinal BA sequestration activates both classic and alternative BA synthesis pathways (45, 46). A similar improvement in metabolic parameters was also observed in apical sodium dependent bile acid transporter (ASBT) inhibitor-treated WD-fed mice where inhibition of intestinal BA reuptake was associated with increased BA biosynthesis (47). These data suggest that inhibition of intestinal BA reuptake improves metabolic parameters by increasing hepatic BA biosynthesis. Alternatively, it is possible that the ability of sevelamer to bind lipids or alter intestinal lipid absorption via neutralization of intestinal BAs may also contribute to the improvement in metabolic derangements in sevelamer treated WD-fed mice. Since, intestinal BA critically regulates hepatic BA synthesis and whole-body metabolism (48-50), further studies are needed to delineate how alterations in the composition of the colonic BA pool or sequestration of intestinal BAs modulates lipid absorption and intestinal BA receptor expression, and to determine their effects on hepatic BA synthesis.

The modest outcomes of recent early phase clinical trials for NASH with fibrosis that are examining efficacy of various nuclear hormone receptor modulators, fatty acid synthesis inhibitors, anti-apoptotic drugs, anti-fibrotics, and immunomodulators, as well as drugs used for T2DM and autoimmune diseases, demonstrate the complexity to finding effective long-term treatments for NASH (51). There is a significant resurgence in interest in BAs as crucial players mediating metabolism of carbohydrates and lipids as well as in hepatic inflammation and fibrosis. Therefore, further studies are needed to fully understand the respective mechanistic contributions of BAs not-only with respect to regulation of lipid and carbohydrate metabolism, but also with respect to intestinal epithelial permeability, cellular injury and repair, as well as hepatic inflammation and fibrosis.

Acknowledgements. This research project was supported in part by the University of Pittsburgh Biospecimen Processing and Repository Core and Advanced Cell and Tissue imaging Centre of the Pittsburgh Liver Research Centre supported by NIH/NIDDK Digestive Disease Research Core Center grant P30DK120531; Emory University Integrated Cellular Imaging Microscopy Core of the Emory and Children's Pediatric Research Center, and the Emory Integrated Lipidomics Core.

526

527 **FIGURE LEGENDS**

528 ***Figure 1. NASH development in western diet fed mice is associated with increased***
529 ***colonic bile acids.*** Photomicrographs of (**A**) Hematoxylin and Eosin (H&E) and (**B**)
530 Serius Red stained liver tissue sections of *F11r*$^{-/-}$ mice fed a normal chow (ND) or
531 western diet (WD) for 16 weeks (n = 5). Scale bar 20 µm. Black arrowhead, collagen
532 deposition in the liver. (**C-F**) Quantitative reverse transcription PCR analysis of hepatic
533 (**C**) α smooth muscle actin (αSMA), (**D**) tissue inhibitor of metalloproteinases (TIMP)-1,
534 (**E**) collagen I αI, and (**F**) collagen I αII transcripts. Serum (**G**) ALT and (**H**) AST levels.
535 (**I**) Total bile acid (BA) in the cecal content, and (**J-K**) composition of cecal BAs. CDCA,
536 chenodeoxycholic acid; CA, cholic acid; MCA, muricholic acid; UDCA, ursodeoxycholic
537 acid; DCA, deoxycholic acid; LCA, lithocholic acid; TCA, taurocholic acid; TLCA,
538 taurolithocholic acid; TDCA, taurodeoxycholic acid; TCDCA,
539 taurochenodeoxycholic acid; THDCA, taurohyodeoxycholic acid and TUDCA,
540 tauroursodeoxycholic acid. Data are presented as means ± SEM. * $p < 0.05$ ND vs WD-
541 fed mice.

542

543 ***Figure 2. Sevelamer protects epithelial barrier from bile acid–induced increase in***
544 ***paracellular permeability.*** (**A-B**) Paracellular flux of 4 kDa FITC-Dextran across a
545 Caco2 monolayer treated with individual bile acid (BAs) or BAs mixed with sevelamer
546 (Sev). Fully differentiated Caco-2 cell monolayers were treated with individual BAs or
547 BAs premixed with sevelamer for 2 hrs in the presence of 4 kDa FITC-Dextran. FITC-
548 dextran flux was determined by measuring fluorescence intensity of media in the basal
549 chamber. (**C-D**) Transepithelial electrical resistance (TEER) of Caco2 monolayers treated
550 with individual BAs, or BAs mixed with sevelamer. TEER was measured before adding
551 BAs and again after 2-hr incubation. TEER readings are reported as the normalized
552 values after 2-hr incubation. (**E**) Fold change in intestinal permeability to FITC-dextran
553 in control and CDCA-fed mice (n = 3 - 4 mice per cohort). CA, cholic acid; CDCA,
554 chenodeoxycholic acid; TCA, taurocholic acid; TDCA, taurodeoxycholic acid; and LCA,
555 lithocholic acid. Data are representative means ± SEM of at least 4 individual monolayer
556 inserts. * $p < 0.05$ HBSS or methanol vs BA treated wells. # $p < 0.05$ BA vs BA plus

sevelamer-treated wells.

Figure 3. Sequestration of intestinal bile acids improves epithelial barrier in western diet fed mice. (**A**) Study design. Mice were fed a normal chow (ND) or western diet (WD) for 12 weeks followed by either the ND or WD with or without sevelamer (Sev) for an additional four weeks (n = 5 mice per cohort). (**B**) Total bile acid (BA) in the cecal content, and (**C**) composition of cecal BAs. CDCA, chenodeoxycholic acid; CA, cholic acid; MCA, muricholic acid; UDCA, ursodeoxycholic acid; DCA, deoxycholic acid; LCA, lithocholic acid; TCA, taurocholic acid; TLCA, taurolithocholic acid; TDCA, taurodeoxycholic acid; TCDCA, taurochenodeoxycholic acid; THDCA, taurohyodeoxycholic acid and TUDCA, tauroursodeoxycholic acid. Data are presented as means ± SEM. * $p < 0.05$ ND vs WD fed mice. # $p < 0.05$ between control and sevelamer treated mice. (**D-G**) Confocal microscopic images with quantification of (**D-E**) occludin and (**F-G**) ZO-1 immunofluorescence in the colonic tissue. Scale bar 20 μm.

Figure. 4. Intestinal bile acid sequestration attenuates western diet-induced mucosal inflammation. (**A**) Photomicrographs of Hematoxylin and Eosin (H&E) stained colonic mucosal tissue sections of *F11r*$^{-/-}$ mice fed a normal chow (ND) or western diet (WD) for 12 weeks followed by either the ND or WD with or without sevelamer (Sev) for an additional four weeks (n = 5 mice per cohort). Scale bar 20 μm. Black arrowhead, immune cell infiltration. (**B-C**) Confocal microscopic images of (**B**) myeloperoxidase (MPO) and (**C**) Ly6G expression in the colonic tissue. Scale bar 20 μm. (**D-E**) Quantitative reverse transcription PCR analysis (RT-PCR) of colonic (**D**) TNFα and (**E**) IL1β transcripts. Data are presented as means ± SEM. * $p < 0.05$ ND vs. WD fed mice. $^{\#}p < 0.05$ control vs. sevelamer treated mice.

Figure. 5. Sequestration of intestinal bile acids protects mice from western diet-induced hepatic inflammation and fibrosis. Photomicrographs of (**A**) Hematoxylin and Eosin (H&E) stained liver tissue sections of *F11r*$^{-/-}$ mice fed a normal chow (ND) or western diet (WD) for 12 weeks followed by either the ND or WD with or without sevelamer (Sev) for an additional four weeks (n = 5 mice per cohort). Scale bar 20 μm.

(**B, C**) Serum (**B**) ALT and (**C**) AST levels. (**D-F**) Quantification of hepatic proinflammatory cytokines (**D**) TNFα, (**E**) IL-1β and (**F**) IL-6. Photomicrographs of (**G**) Sirius Red stained liver tissue sections. Scale bar 20 μm. Black arrowhead, collagen deposition in the liver. (**H-K**) Quantitative reverse transcription PCR (RT-PCR) analysis of hepatic (**H**) α smooth muscle actin (αSMA), (**I**) tissue inhibitor of metalloproteinase (TIMP)-1, (**J**) collagen IαI and (**K**) collagen IαII transcripts. (**L**) Confocal microscopic images of tissue resident macrophage marker F4/80 expression in the liver. Scale bar 20 μm. (**M-P**) RT-PCR analysis of hepatic (**M**) F4/80, (**N**) monocyte chemoattractant protein (MCP)-1, (**O**) CD68 and (**P**) C-C chemokine receptor (CCR)-2 transcripts. Data are presented as means ± SEM. *$p < 0.05$ ND vs. WD fed mice. $^{\#}$ $p < 0.05$ control vs. sevelamer treated mice.

Figure. 6. Intestinal bile acid sequestration improves metabolic parameters and glucose homeostasis. (**A**) Changes in body, (**B**) liver, and (**C**) visceral fat weight in *F11r*$^{-/-}$ mice fed a normal chow (ND) or western diet (WD) for 12 weeks followed by either the ND or WD with or without sevelamer (Sev) for an additional four weeks (n = 5 mice per cohort). Changes in the liver and visceral fat weights are reported as percent of body weight. (**D**) Glucose, and (**E**) insulin tolerance after 16 weeks of total feeding. (**F**) Changes in serum cholesterol levels. Confocal microscopic images of (**G**) BODIPY (lipids) stained liver tissue sections. Scale bar 20 μm. (**H**) Average daily calorie intake. Data are presented as means ± SEM. * $p < 0.05$ ND vs. WD fed mice. # $p < 0.05$ control vs. sevelamer treated mice.

Figure. 7. Intestinal bile acid sequestration restores western diet-induced alterations in hepatic BA pool. (**A**) Total hepatic BA content and (**B**) composition in mice fed a normal chow (ND) or western diet (WD) for 12 weeks followed by either the ND or WD with or without sevelamer (Sev) for an additional four weeks (n = 5 mice per cohort). CDCA, chenodeoxycholic acid; CA, cholic acid; MCA, muricholic acid; UDCA, ursodeoxycholic acid; DCA, deoxycholic acid; LCA, lithocholic acid; TCA, taurocholic acid; TLCA, taurolithocholic acid; TDCA, taurodeoxycholic acid; TCDCA, taurochenodeoxycholic acid; THDCA, taurohyodeoxycholic acid and TUDCA,

tauroursodeoxycholic acid. (**C-E**) RT-PCR analysis of (**C**) *CYP7A1*, (**D**) *CYP27A1* and (**E**) *CYP7B1* transcripts in the liver. Data are presented as means ± SEM. * $p < 0.05$ ND vs. WD fed mice. # $p < 0.05$ control vs. sevelamer treated mice.

Figure. 8. Western diet increases the abundance of gut microbial taxa associated with bile acid metabolism. (**A**) Microbiota richness and diversity in the colonic mucosa in mice fed a normal chow (ND) or western diet (WD) for 12 weeks followed by either the ND or WD with or without sevelamer (Sev) for an additional four weeks (n = 3-5 mice per cohort). (**B**) Jackknifed principal coordinate analysis (PCoA) of the un-weighted UniFrac distance matrix of the colonic mucosa-associated microbiota. Symbols represent data from individual mice color-coded by the indicated metadata. The ovals represent clustering by treatment groups. (**C**) Relative abundance of bacterial orders in the colonic mucosa. Bars represent individual mice. Labels indicate families with average relative abundances ≥1% in at least one treatment group. (**D**) Relative abundance of mucosa-associated bacterial families significantly altered in WD or WD plus sevelamer treated mice. Data are presented as means ± SEM. * $p < 0.05$ ND vs. WD fed mice. # $p < 0.05$ control vs. sevelamer treated mice.

REFERENCES

1. Schuppan, D., and Schattenberg, J. M. (2013) Non-alcoholic steatohepatitis: pathogenesis and novel therapeutic approaches. *J Gastroenterol Hepatol* **28 Suppl 1**, 68-76
2. Kanwal, F., Kramer, J. R., Mapakshi, S., Natarajan, Y., Chayanupatkul, M., Richardson, P. A., Li, L., Desiderio, R., Thrift, A. P., Asch, S. M., Chu, J., and El-Serag, H. B. (2018) Risk of Hepatocellular Cancer in Patients With Non-Alcoholic Fatty Liver Disease. *Gastroenterology* **155**, 1828-1837 e1822

3. Estes, C., Razavi, H., Loomba, R., Younossi, Z., and Sanyal, A. J. (2018) Modeling the epidemic of nonalcoholic fatty liver disease demonstrates an exponential increase in burden of disease. *Hepatology* **67**, 123-133
4. Adams, L. A., Lymp, J. F., St Sauver, J., Sanderson, S. O., Lindor, K. D., Feldstein, A., and Angulo, P. (2005) The natural history of nonalcoholic fatty liver disease: a population-based cohort study. *Gastroenterology* **129**, 113-121
5. O'Grady, M. J. a. C., J.C. (2012) Assessing the Economics of Obesity and Obesity Interventions. pp. 1-40
6. Wigg, A. J., Roberts-Thomson, I. C., Dymock, R. B., McCarthy, P. J., Grose, R. H., and Cummins, A. G. (2001) The role of small intestinal bacterial overgrowth, intestinal permeability, endotoxaemia, and tumour necrosis factor alpha in the pathogenesis of non-alcoholic steatohepatitis. *Gut* **48**, 206-211
7. Miele, L., Valenza, V., La Torre, G., Montalto, M., Cammarota, G., Ricci, R., Masciana, R., Forgione, A., Gabrieli, M. L., Perotti, G., Vecchio, F. M., Rapaccini, G., Gasbarrini, G., Day, C. P., and Grieco, A. (2009) Increased intestinal permeability and tight junction alterations in nonalcoholic fatty liver disease. *Hepatology* **49**, 1877-1887
8. Luther, J., Garber, J. J., Khalili, H., Dave, M., Bale, S. S., Jindal, R., Motola, D. L., Luther, S., Bohr, S., Jeoung, S. W., Deshpande, V., Singh, G., Turner, J. R., Yarmush, M. L., Chung, R. T., and Patel, S. J. (2015) Hepatic Injury in Nonalcoholic Steatohepatitis Contributes to Altered Intestinal Permeability. *Cell Mol Gastroenterol Hepatol* **1**, 222-232
9. Rahman, K., Desai, C., Iyer, S. S., Thorn, N. E., Kumar, P., Liu, Y., Smith, T., Neish, A. S., Li, H., Tan, S., Wu, P., Liu, X., Yu, Y., Farris, A. B., Nusrat, A., Parkos, C. A., and Anania, F. A. (2016) Loss of Junctional Adhesion Molecule A Promotes Severe Steatohepatitis in Mice on a Diet High in Saturated Fat, Fructose, and Cholesterol. *Gastroenterology*
10. Chiang, J. Y. (2009) Bile acids: regulation of synthesis. *J Lipid Res* **50**, 1955-1966
11. Chiang, J. Y. (2017) Recent advances in understanding bile acid homeostasis. *F1000Res* **6**, 2029

12. Ridlon, J. M., Kang, D. J., Hylemon, P. B., and Bajaj, J. S. (2014) Bile acids and the gut microbiome. *Curr Opin Gastroenterol* **30**, 332-338
13. Ramirez-Perez, O., Cruz-Ramon, V., Chinchilla-Lopez, P., and Mendez-Sanchez, N. (2017) The Role of the Gut Microbiota in Bile Acid Metabolism. *Ann Hepatol* **16**, s15-s20
14. Wahlstrom, A., Sayin, S. I., Marschall, H. U., and Backhed, F. (2016) Intestinal Crosstalk between Bile Acids and Microbiota and Its Impact on Host Metabolism. *Cell Metab* **24**, 41-50
15. Dawson, P. A., and Karpen, S. J. (2015) Intestinal transport and metabolism of bile acids. *J Lipid Res* **56**, 1085-1099
16. Camilleri, M. (2015) Bile Acid diarrhea: prevalence, pathogenesis, and therapy. *Gut Liver* **9**, 332-339
17. Oduyebo, I., and Camilleri, M. (2017) Bile acid disease: the emerging epidemic. *Curr Opin Gastroenterol* **33**, 189-195
18. Staley, C., Weingarden, A. R., Khoruts, A., and Sadowsky, M. J. (2017) Interaction of gut microbiota with bile acid metabolism and its influence on disease states. *Appl Microbiol Biotechnol* **101**, 47-64
19. Barrasa, J. I., Olmo, N., Lizarbe, M. A., and Turnay, J. (2013) Bile acids in the colon, from healthy to cytotoxic molecules. *Toxicol In Vitro* **27**, 964-977
20. Stenman, L. K., Holma, R., Eggert, A., and Korpela, R. (2013) A novel mechanism for gut barrier dysfunction by dietary fat: epithelial disruption by hydrophobic bile acids. *Am J Physiol Gastrointest Liver Physiol* **304**, G227-234
21. Sarathy, J., Detloff, S. J., Ao, M., Khan, N., French, S., Sirajuddin, H., Nair, T., and Rao, M. C. (2017) The Yin and Yang of bile acid action on tight junctions in a model colonic epithelium. *Physiol Rep* **5**, e13294
22. Raimondi, F., Santoro, P., Barone, M. V., Pappacoda, S., Barretta, M. L., Nanayakkara, M., Apicella, C., Capasso, L., and Paludetto, R. (2008) Bile acids modulate tight junction structure and barrier function of Caco-2 monolayers via EGFR activation. *Am J Physiol Gastrointest Liver Physiol* **294**, G906-913

23. Araki, Y., Katoh, T., Ogawa, A., Bamba, S., Andoh, A., Koyama, S., Fujiyama, Y., and Bamba, T. (2005) Bile acid modulates transepithelial permeability via the generation of reactive oxygen species in the Caco-2 cell line. *Free Radic Biol Med* **39**, 769-780
24. Munch, A., Soderholm, J. D., Ost, A., Carlsson, A. H., Magnusson, K. E., and Strom, M. (2011) Low levels of bile acids increase bacterial uptake in colonic biopsies from patients with collagenous colitis in remission. *Aliment Pharmacol Ther* **33**, 954-960
25. Munch, A., Strom, M., and Soderholm, J. D. (2007) Dihydroxy bile acids increase mucosal permeability and bacterial uptake in human colon biopsies. *Scand J Gastroenterol* **42**, 1167-1174
26. Mouzaki, M., Wang, A. Y., Bandsma, R., Comelli, E. M., Arendt, B. M., Zhang, L., Fung, S., Fischer, S. E., McGilvray, I. G., and Allard, J. P. (2016) Bile Acids and Dysbiosis in Non-Alcoholic Fatty Liver Disease. *PLoS One* **11**, e0151829
27. Chopyk, D. M., Kumar, P., Raeman, R., Liu, Y., Smith, T., and Anania, F. A. (2017) Dysregulation of junctional adhesion molecule-A contributes to ethanol-induced barrier disruption in intestinal epithelial cell monolayers. *Physiol Rep* **5**
28. Friedman, S. L. (2008) Hepatic stellate cells: protean, multifunctional, and enigmatic cells of the liver. *Physiol Rev* **88**, 125-172
29. Hidalgo, I. J., Raub, T. J., and Borchardt, R. T. (1989) Characterization of the human colon carcinoma cell line (Caco-2) as a model system for intestinal epithelial permeability. *Gastroenterology* **96**, 736-749
30. Braunlin, W., Zhorov, E., Guo, A., Apruzzese, W., Xu, Q., Hook, P., Smisek, D. L., Mandeville, W. H., and Holmes-Farley, S. R. (2002) Bile acid binding to sevelamer HCl. *Kidney Int* **62**, 611-619
31. McGettigan, B. M., McMahan, R. H., Luo, Y., Wang, X. X., Orlicky, D. J., Porsche, C., Levi, M., and Rosen, H. R. (2016) Sevelamer Improves Steatohepatitis, Inhibits Liver and Intestinal Farnesoid X Receptor (FXR), and Reverses Innate Immune Dysregulation in a Mouse Model of Non-alcoholic Fatty Liver Disease. *J Biol Chem* **291**, 23058-23067

32. Sayin, S. I., Wahlstrom, A., Felin, J., Jantti, S., Marschall, H. U., Bamberg, K., Angelin, B., Hyotylainen, T., Oresic, M., and Backhed, F. (2013) Gut microbiota regulates bile acid metabolism by reducing the levels of tauro-beta-muricholic acid, a naturally occurring FXR antagonist. *Cell Metab* **17**, 225-235
33. Ridlon, J. M., Kang, D. J., and Hylemon, P. B. (2006) Bile salt biotransformations by human intestinal bacteria. *J Lipid Res* **47**, 241-259
34. Jones, B. V., Begley, M., Hill, C., Gahan, C. G., and Marchesi, J. R. (2008) Functional and comparative metagenomic analysis of bile salt hydrolase activity in the human gut microbiome. *Proc Natl Acad Sci U S A* **105**, 13580-13585
35. Devkota, S., Wang, Y., Musch, M. W., Leone, V., Fehlner-Peach, H., Nadimpalli, A., Antonopoulos, D. A., Jabri, B., and Chang, E. B. (2012) Dietary-fat-induced taurocholic acid promotes pathobiont expansion and colitis in Il10-/- mice. *Nature* **487**, 104-108
36. Hegyi, P., Maleth, J., Walters, J. R., Hofmann, A. F., and Keely, S. J. (2018) Guts and Gall: Bile Acids in Regulation of Intestinal Epithelial Function in Health and Disease. *Physiol Rev* **98**, 1983-2023
37. Ignacio Barrasa, J., Olmo, N., Perez-Ramos, P., Santiago-Gomez, A., Lecona, E., Turnay, J., and Antonia Lizarbe, M. (2011) Deoxycholic and chenodeoxycholic bile acids induce apoptosis via oxidative stress in human colon adenocarcinoma cells. *Apoptosis* **16**, 1054-1067
38. Debruyne, P. R., Bruyneel, E. A., Li, X., Zimber, A., Gespach, C., and Mareel, M. M. (2001) The role of bile acids in carcinogenesis. *Mutat Res* **480-481**, 359-369
39. Bernstein, C., Holubec, H., Bhattacharyya, A. K., Nguyen, H., Payne, C. M., Zaitlin, B., and Bernstein, H. (2011) Carcinogenicity of deoxycholate, a secondary bile acid. *Arch Toxicol* **85**, 863-871
40. Narushima, S., Ito, K., Kuruma, K., and Uchida, K. (2000) Composition of cecal bile acids in ex-germfree mice inoculated with human intestinal bacteria. *Lipids* **35**, 639-644

41. Narushima, S., Itoha, K., Miyamoto, Y., Park, S. H., Nagata, K., Kuruma, K., and Uchida, K. (2006) Deoxycholic acid formation in gnotobiotic mice associated with human intestinal bacteria. *Lipids* **41**, 835-843
42. Kitahara, M., Takamine, F., Imamura, T., and Benno, Y. (2000) Assignment of Eubacterium sp. VPI 12708 and related strains with high bile acid 7alpha-dehydroxylating activity to Clostridium scindens and proposal of Clostridium hylemonae sp. nov., isolated from human faeces. *Int J Syst Evol Microbiol* **50 Pt 3**, 971-978
43. Li, T., Francl, J. M., Boehme, S., and Chiang, J. Y. (2013) Regulation of cholesterol and bile acid homeostasis by the cholesterol 7alpha-hydroxylase/steroid response element-binding protein 2/microRNA-33a axis in mice. *Hepatology* **58**, 1111-1121
44. Li, T., Owsley, E., Matozel, M., Hsu, P., Novak, C. M., and Chiang, J. Y. (2010) Transgenic expression of cholesterol 7alpha-hydroxylase in the liver prevents high-fat diet-induced obesity and insulin resistance in mice. *Hepatology* **52**, 678-690
45. Thomas, C., Pellicciari, R., Pruzanski, M., Auwerx, J., and Schoonjans, K. (2008) Targeting bile-acid signalling for metabolic diseases. *Nat Rev Drug Discov* **7**, 678-693
46. Russell, D. W. (2003) The enzymes, regulation, and genetics of bile acid synthesis. *Annu Rev Biochem* **72**, 137-174
47. Rao, A., Kosters, A., Mells, J. E., Zhang, W., Setchell, K. D., Amanso, A. M., Wynn, G. M., Xu, T., Keller, B. T., Yin, H., Banton, S., Jones, D. P., Wu, H., Dawson, P. A., and Karpen, S. J. (2016) Inhibition of ileal bile acid uptake protects against nonalcoholic fatty liver disease in high-fat diet-fed mice. *Sci Transl Med* **8**, 357ra122
48. Fang, S., Suh, J. M., Reilly, S. M., Yu, E., Osborn, O., Lackey, D., Yoshihara, E., Perino, A., Jacinto, S., Lukasheva, Y., Atkins, A. R., Khvat, A., Schnabl, B., Yu, R. T., Brenner, D. A., Coulter, S., Liddle, C., Schoonjans, K., Olefsky, J. M., Saltiel, A. R., Downes, M., and Evans, R. M. (2015) Intestinal FXR agonism promotes

adipose tissue browning and reduces obesity and insulin resistance. *Nat Med* **21**, 159-165

49. Li, F., Jiang, C., Krausz, K. W., Li, Y., Albert, I., Hao, H., Fabre, K. M., Mitchell, J. B., Patterson, A. D., and Gonzalez, F. J. (2013) Microbiome remodelling leads to inhibition of intestinal farnesoid X receptor signalling and decreased obesity. *Nat Commun* **4**, 2384

50. Drucker, D. J. (2001) Minireview: the glucagon-like peptides. *Endocrinology* **142**, 521-527

51. Lemoinne, S., and Friedman, S. L. (2019) New and emerging anti-fibrotic therapeutics entering or already in clinical trials in chronic liver diseases. *Curr Opin Pharmacol* **49**, 60-70

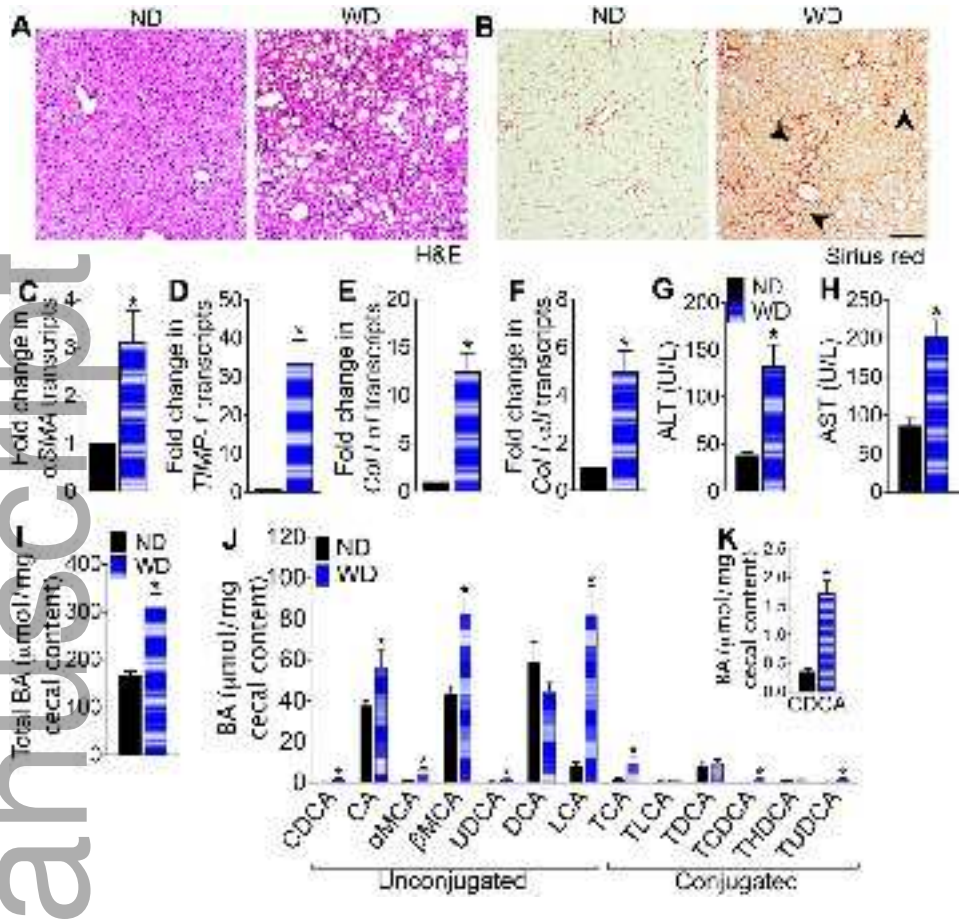

fsb2_20488_f1.tif

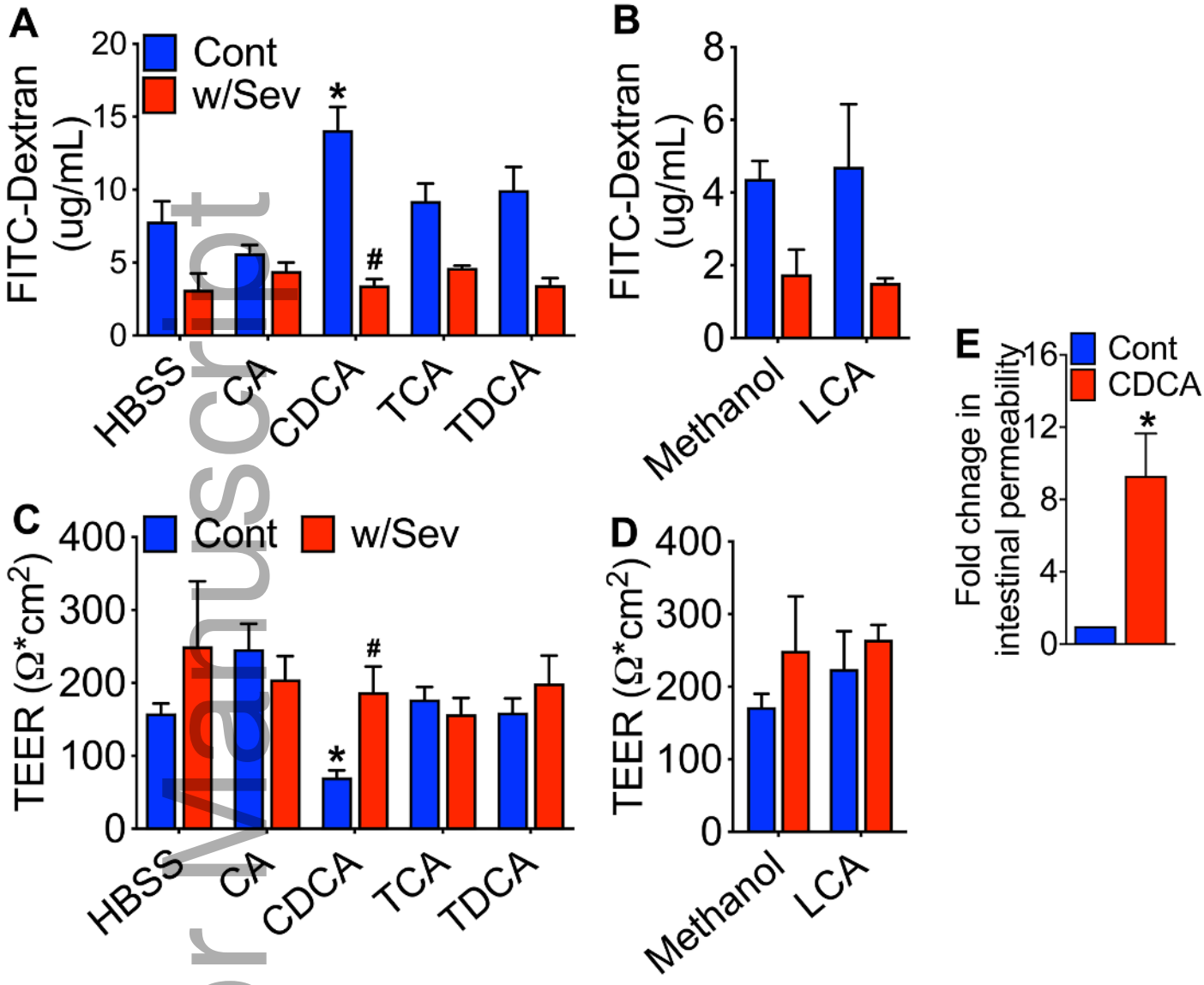

fsb2_20488_f2.tif

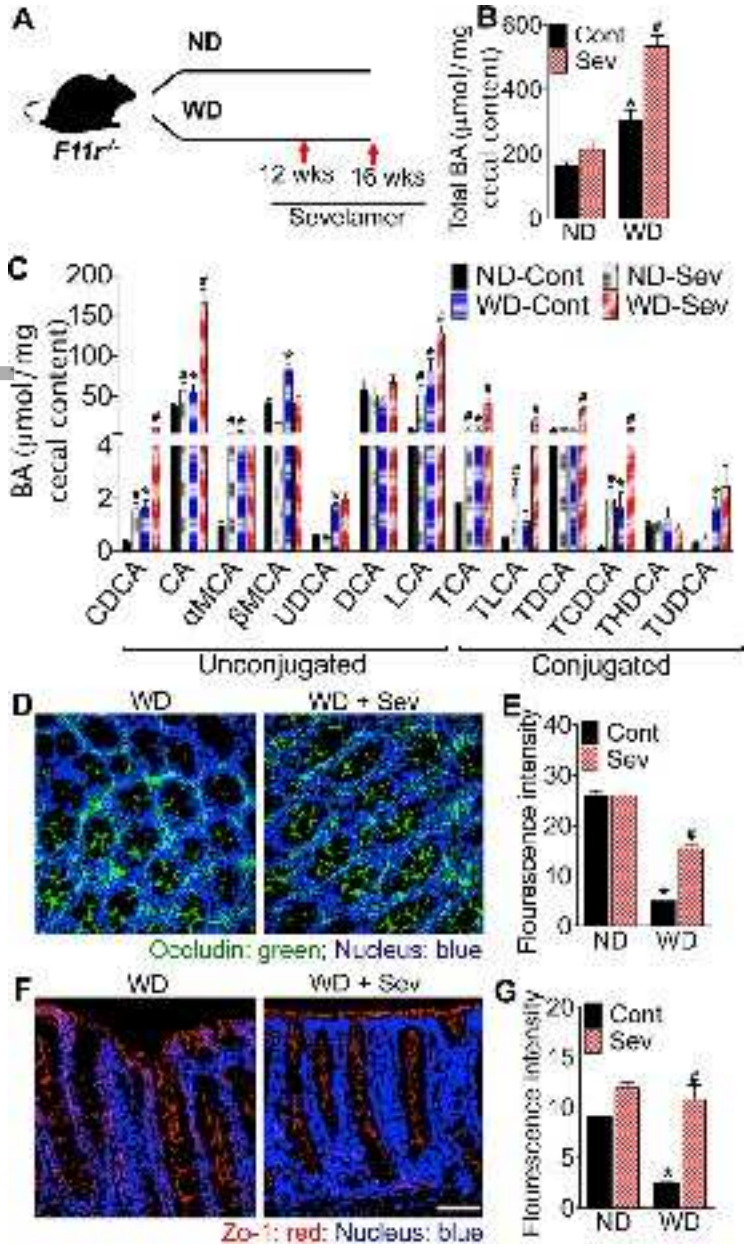

fsb2_20488_f3.tif

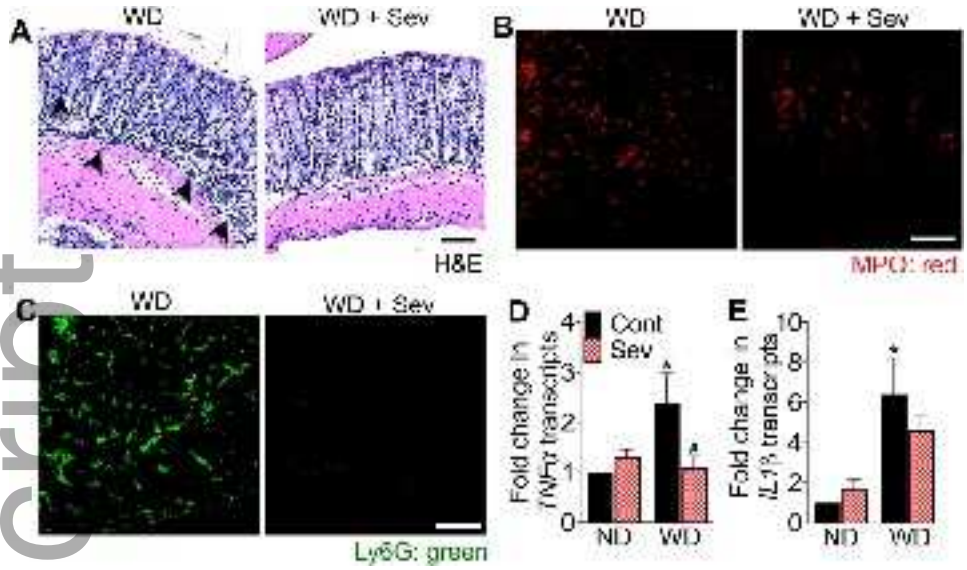

fsb2_20488_f4.tif

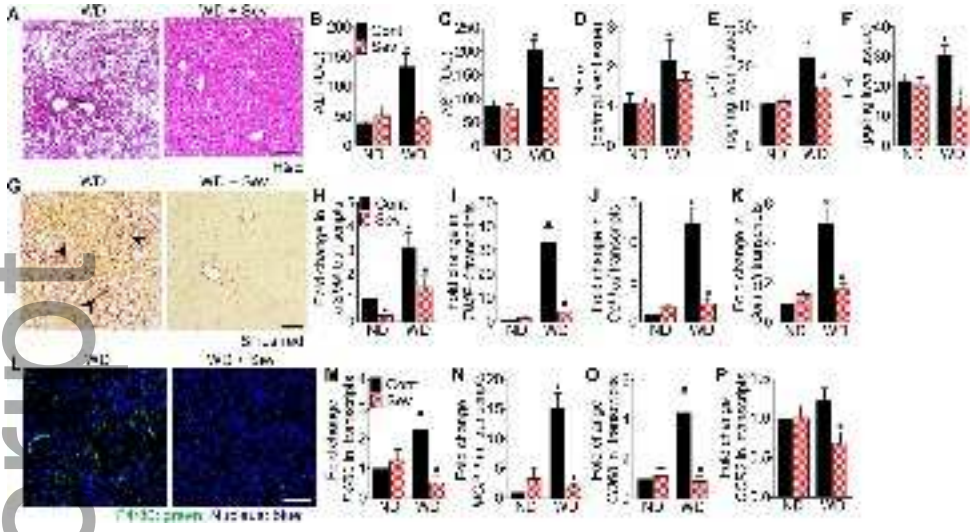

fsb2_20488_f5.tif

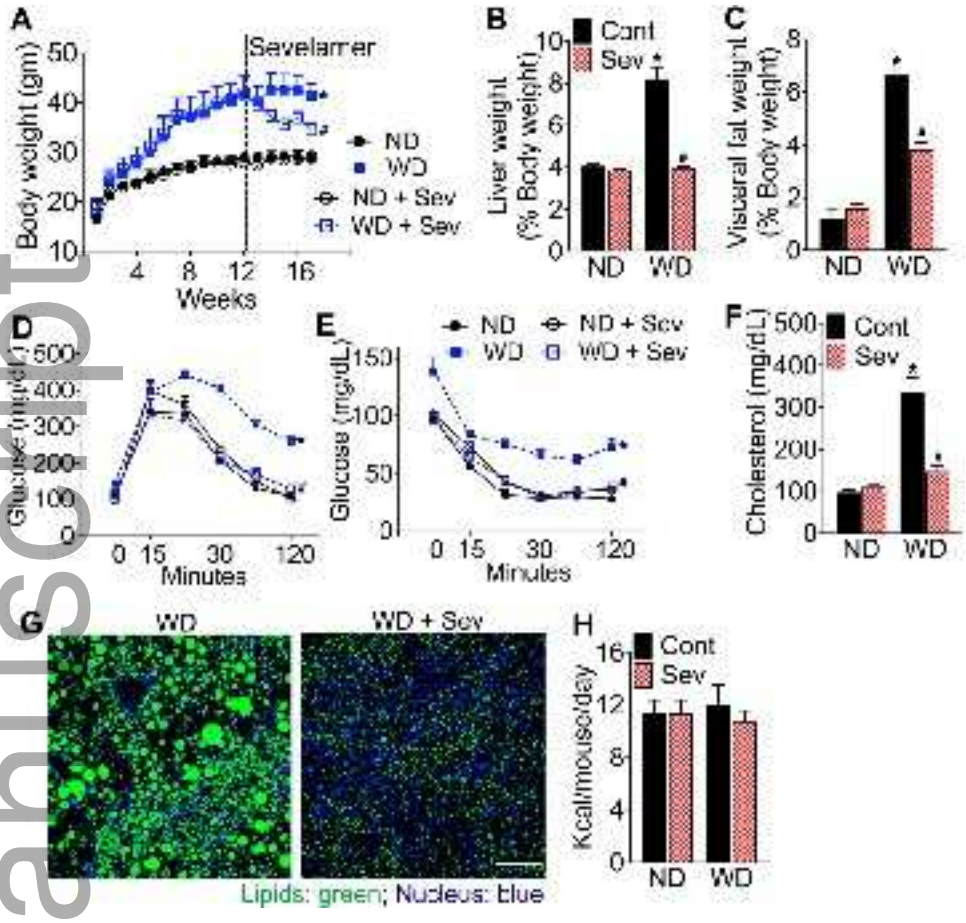

fsb2_20488_f6.tif

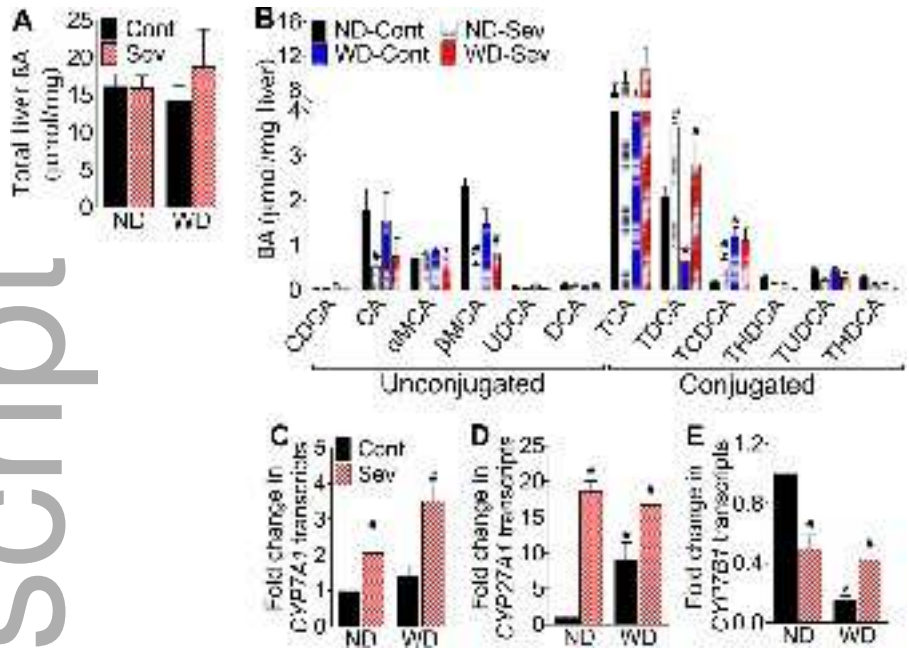

fsb2_20488_f7.tif

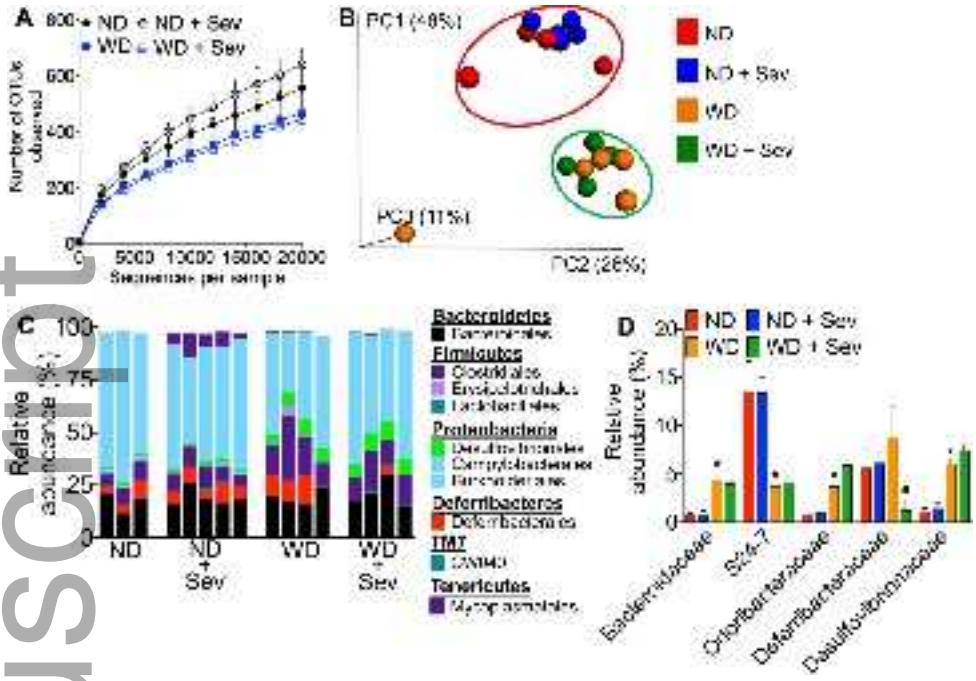

fsb2_20488_f8.tif